ELSEVIER

Journal of Supercritical Fluids 14 (1998) 55–65

THE JOURNAL OF
Supercritical
Fluids

Processing of epoxy resins using carbon dioxide as an antisolvent

K.J. Heater [a], D.L. Tomasko [b,*]

[a] *METSS Corporation, 720-G Lakeview Plaza Blvd, Columbus, OH 43085, USA*
[b] *Department of Chemical Engineering, The Ohio State University, 140 W. 19th Ave., Columbus, OH 43210, USA*

Received 24 September 1997; received in revised form 25 April 1998; accepted 27 April 1998

Abstract

The use of carbon dioxide as an antisolvent for the production of polymeric particles is well documented. However, development of operating parameters to control particle size and morphology in this process has been generally lacking. In an attempt to gain a better understanding of processing conditions on particle formation, we present results on precipitation of epoxy resin powders with and without surfactants in the liquid phase including a comparison of cocurrent and countercurrent flow configurations and higher solute concentrations for increased throughput. It can be inferred from the results that for this system, mixing, nucleation, and growth phenomena in the precipitation chamber are more significant than the jet break-up effects created by the kinetic energy of the liquid solution as it is forced through the nozzle. © 1998 Elsevier Science B.V. All rights reserved.

Keywords: Antisolvent precipitation; Carbon dioxide; Epoxy resin ; Mixing; Surfactants

---

1. Introduction

Significant efforts are underway to incorporate carbon dioxide as an environmentally benign solvent in many aspects of polymer processing. One of these processes is the production of polymeric powders in uniform spherical morphologies with a tight size distribution. Since the introduction of supercritical antisolvent techniques for the comminution of solid materials nearly a decade ago [1,2], there have been many attempts to achieve precise control over particle size and morphology. To date, however, as with many supercritical technologies, specific guidelines for operating parameters are unavailable and much experimentation is required on any new system to establish such parameters.

There are two typical methods using supercritical antisolvents to precipitate polymers: (1) carbon dioxide (or other antisolvent) can be injected into a vessel containing a liquid solution from which a solute is to be precipitated; or (2) the liquid solution can be sprayed through a nozzle into a vessel containing the antisolvent. These methods are referred to in the literature as gas antisolvent (GAS), supercritical antisolvent (SAS), or precipitation with a compressed fluid antisolvent (PCA) and differ from the rapid expansion of supercritical solutions (RESS) process due to the presence of a liquid solvent as a separate phase. We are most interested in the spray process and our experiments are most similar to those referred to as PCA since we use liquid CO_2 as the antisolvent.

---

* Corresponding author. Tel: 00 1 614 292 4249;
Fax: 00 1 614 292 3769; e-mail: tomasko.1@osu.edu

0896-8446/98/$ – see front matter
PII S0896-8446(98)00106-5

General trends of various effects have been reported for processing including temperature, pressure, nozzle size, flow rate, and concentration of solute. Because the precipitation appears to be dominated by mass transfer (or physical) effects, it has not been possible to discern the effect (if any) of thermodynamic solution non-idealities on particle formation. Also, while literature is available on solutes other than polymers (e.g. pharmaceuticals or proteins) [3–5], it is not presently possible to infer information from those studies because the different solution properties (solute molecular weight, viscosity, and concentration) give rise to radically different nucleation and growth rates.

In supercritical fluid studies, the density of the fluid is usually given the most attention when characterizing the process since it can be altered continuously over a wide range. In previous studies of dilute polymer solutions, the effect of density has resulted in ambiguous conclusions. One study of a semi-crystalline polymer (poly-L-lactic acid) in methylene chloride showed that particle size decreased with increasing pressure (density) up to the critical pressure, above which particle size increased with pressure [6]. A separate study of non-crystalline polystyrene in toluene showed that particle size decreased with increasing pressure (density) [7]. The latter group also made significant use of the liquid CO_2 state to produce a wide array of particle morphologies such as microballoons and microcellular porous microspheres [8]. In addition to the processing parameters, the structure of the polymer can have an impact on the morphology of the particles obtained. For a highly crystalline polyamide, highly oriented fibrils were obtained for quite dilute solutions of polymer in the liquid solvent (<0.1 wt%) [9]. At similar processing conditions, the non-crystalline or semi-crystalline polymers form amorphous spherical morphologies. In fact, the particle morphology could be changed from small crystallites to fibers by altering only the polymer structure [10]. Of the studies carried out with low solution concentrations, there appears to be some consensus that mass transfer of the CO_2 into the liquid and vice versa has a much more significant effect on particle size and morphology than the hydrodynamics of the liquid jet break-up. The ambiguities mentioned above can be explained in terms of different mass transfer rates of the liquid solvents. Our results are in agreement with this conclusion.

From a processing standpoint, it is desirable to increase throughput by working with more concentrated solutions. In general, increasing the concentration of polymer in the liquid solution over approximately 4 wt% has been shown to lead to the formation of fibers or continuous networks.[6,11] This is attributed to both the stabilizing affect of the higher solution viscosity on the liquid jet and the changing position of the starting solution relative to the binodal curve in the polymer–solvent–antisolvent phase diagram. In addition, even at conditions where particles are formed, agglomeration of particles is an ubiquitous problem due to the plasticization of many polymers by carbon dioxide. Johnston and coworkers have recently described the use of stabilizing surfactants to avoid this problem [12,13].

2. Experimental

Two types of apparatus were used in this work. Solvent expansion studies were used to screen operating conditions and confirm liquid solvent compatibility with CO_2. For this, a simple Jerguson gauge attached to a CO_2 supply was used. Particle formation studies were carried out in a large 2.75 l vessel fed by two ISCO 260D syringe pumps. The nozzle in the top plug of the vessel was a machined piece of jeweler stone fitted into a length of 1/16 in stainless tubing (Blundell). The nozzle internal design was tapered from 1.17 mm down to 0.18 mm followed by a straight section of 0.18 mm diameter and approximately 0.30 mm length. The nozzle diameters listed in Table 1 refer to the straight section of the nozzle only. The system shown in Fig. 1 could be configured for either cocurrent or countercurrent flow of CO_2 and liquid solution. The vessel was operated at ambient temperature for all studies reported. Pressure was monitored with a pressure transducer (Sensotec AG-300).

The materials used in this study were bone-dry grade CO_2 (Liquid Carbonic), acetone (Parks),

Table 1
Experimental conditions

Solvent	CO_2 pressure (bar)	Epoxy conc. (wt%)	Surf. conc. (wt%)	Solution flow rate (ml min^{-1})	CO_2 flow rate (ml min^{-1})	Nozzle diam. (μm)	Flow configuration
Acetone	95.8	25	0	5	15	150	Co-current
Acetone	95.8	5	0	5	15	150	Co-current
Acetone	95.8	5	0	5	15	150	Co-current
Acetone	95.8	2.5	0	5	10	150	Co-current
Acetone	97.6	2.5	0	5	15	150	Co-current
Acetone	97.6	2.5	0.01	5	15	180	Co-current
Acetone	97.6	25	0.10	5	15	180	Co-current
Acetone	97.6	25	0.01	5	10	180	Co-current
Acetone	83.8	5	0	1	10	180	Co-current
Acetone	97.6	2.5	0.01	5	15	180	Counter-current
Acetone	63.1	2.5	0.01	5	15	180	Co-current
Acetone	97.6	2.5	0.03	1	15	180	Counter-current
Acetone	63.1	2.5	0.02	5	15	180	Counter-current
Acetone	63.1	2.5	0.02	5	15	762	Counter-current
MEK	63.1	10	0	0.5	15	762	Co-current
MEK	63.1	10	0	0.5	15	762	Counter-current
MEK	63.1	2.5	0.02	5	15	180	Co-current
MEK	63.1	2.5	0.02	1	15	180	Co-current
MEK	63.1	2.5	0.02	1	25	180	Counter-current
MEK	63.1	2.5	0.02	0.5	15	180	Co-current
MEK	63.1	2.5	0.025	0.5	25	180	Counter-current
MEK	49.3	10	0.025	0.5	15	180	Counter-current
MEK	97.6	10	0.03	0.5	15	180	Counter-current
MEK	63.1	25	0.035	0.5	15	180	Counter-current

methyl ethyl ketone (MEK) (Parks), and an Epoxy Powder Coating (Corvel 10-1013, Morton). The epoxy contained titanium dioxide, barium sulfate, and a small amount of silica. Slurries of the powder in the organic solvents were prepared and experiments performed using both the slurry (epoxy + inorganic pigment) and the supernatant (epoxy only). To reduce agglomeration, a surfactant stabilizer (Pluronic R-17, BASF) was used in some experiments.

For solvent expansion studies, a known volume of organic solvent was placed in the Jerguson gauge (approximately 300 ml total volume) and a baseline liquid level was recorded. CO_2 was introduced from a syringe pump in increments of 6.9 bar and the system allowed to equilibrate, after which a reading was recorded.

All precipitation studies were carried out by initially filling the vessel with CO_2 at the conditions of interest and establishing a constant flow rate of CO_2 prior to introducing the epoxy solution. The flow of CO_2 through the vessel was either cocurrent or countercurrent to the flow of the liquid solution. After stopping the liquid flow, at least one vessel volume of pure CO_2 at the operating conditions was introduced to remove any excess liquid solvent. Experiments were performed to compare the effect of organic solvent (acetone versus MEK), antisolvent density, concentration of solute, and relative flow rates of solvent and CO_2.

3. Results and discussion

To confirm process conditions wherein the organic solvent becomes miscible with CO_2 [14], solvent expansion experiments were carried out with acetone and MEK. As expected, very little expansion was observed with gaseous CO_2 and a large increase in the liquid phase volume occurred at the vapor pressure of CO_2 (64.3 bar at 25°C).

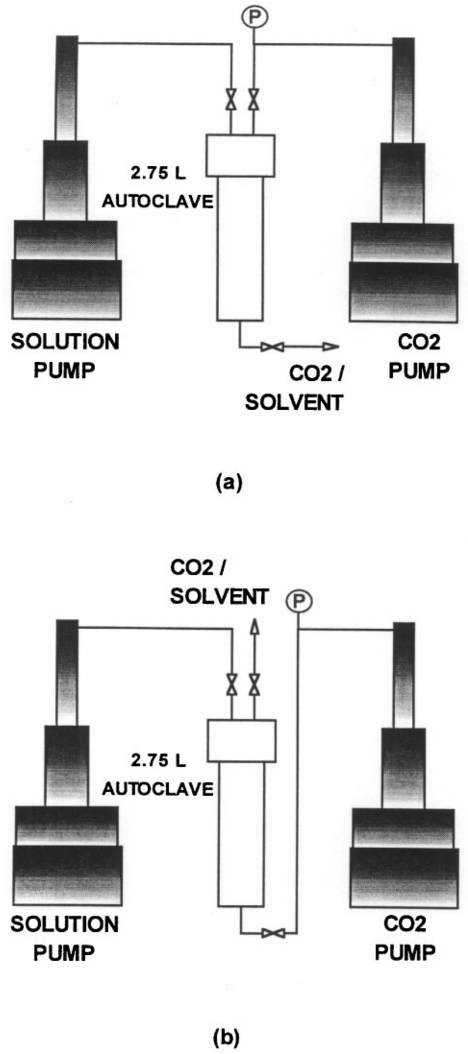

Fig. 1. Schematic of antisolvent precipitation apparatus illustrating: (a) cocurrent; and (b) countercurrent configurations.

To compare the effect of organic solvent on jet break-up, the viscosity of epoxy solutions was measured as a function of concentration at ambient conditions in a Brookfield viscometer. These results are shown in Fig. 2. It is apparent that there is little difference between acetone and MEK until concentrations approach and exceed 50 wt%. The break in the curve at high concentrations is indicative of the transition between dilute and semi-dilute behavior. In the semi-dilute region, there is a dramatic increase in viscosity that results in severe pressure drops across the nozzle in the precipitation experiment. In the subsequent studies, concentrations were kept to 25 wt% or less and therefore the viscosities of the solutions were nearly identical.

Fig. 3 shows an SEM micrograph of the epoxy powder as received. It is characterized by a wide range of particle size and morphology with several particles containing sharp edges. Such morphologies are indicative of mechanical particle grinding. Some of the surface roughness can be attributed the presence of the inorganic pigments.

A series of experiments were carried out as listed in Table 1. The first set of experiments was carried out with various concentrations of epoxy in acetone. The supernatant from solution concentrations of 2.5, 5 and 25 wt% was fed at 5 ml min^{-1} with a co-current flow of CO_2 (5–10 ml min^{-1}) at 1400 psig. The results, shown in Fig. 4, show only precipitated epoxy and indicate two general trends. As the concentration decreases the predominance of rod-like structures in the precipitate decreases in favor of smaller, more spherical structures and the spherical features increase in size in the step from 25 wt% down to 5 wt%. Note that the scale for the 2.5 wt% micrographs is different than that for the higher concentrations. We attribute the rod formation to quick nucleation that ‘freezes’ the shape of the liquid stream exiting the nozzle. As the concentration decreases, nucleation is delayed because more solvent must be removed and in conjunction, the liquid stream is less coherent at the point of nucleation. The viscosity of the 25 wt% solution is approximately 14 cP and that of the 5 wt% solution is 2.5 cP. This also contributes to the greater coherence of the liquid jet at higher concentrations.

Because most of the polymer particles were coalescing to form agglomerates, a small amount (0.1 wt%) of Pluronic R-17 surfactant was added to the liquid solution to deter such agglomeration as shown by Johnston and co-workers [12,13]. The result was a completely uniform spherical morphology that nevertheless still agglomerated (Fig. 5). We believe this agglomeration occurred as a result of the settling of the particles during the pure CO_2 purge. This could be corrected with a better design for collecting particles and optimiz-

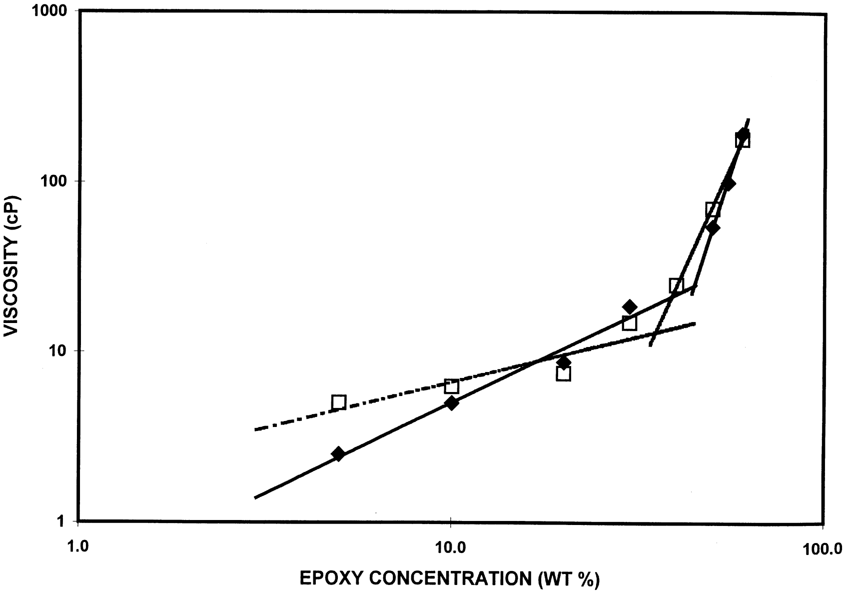

Fig. 2. Viscosity of epoxy solutions in acetone (◆) and MEK (□) at 23°C.

ing flow rates in a scaled-up process. The average particle size increased slightly indicating a longer growth period and more uniform growth mechanism in the presence of surfactant.

Although liquid CO_2 is used, the effect of pressure on the phase behavior of the acetone–CO_2 system is significant. It is also desirable from a processing point of view to operate at the lowest feasible pressure. At the higher pressures shown in Fig. 4, acetone and CO_2 are completely miscible in all proportions at 25°C. In the absence of an interface, there is only diffusional resistance to mass transfer. The transport of acetone in CO_2 should be increased by the reduction in pressure while the transport of CO_2 in the liquid should be relatively unaffected. Therefore, as the pressure is decreased it is expected that the onset of nucleation would be delayed slightly, particularly at the solution–CO_2 interface. Fig. 6 compares the results of different CO_2 pressures on particle morphology and it is seen that the lower pressure with the lower driving force allows more rod-like structures to form. This may be a result of more stable structures precipitating during a longer growth period in a stream that is not sufficiently broken up to yield individual drops.

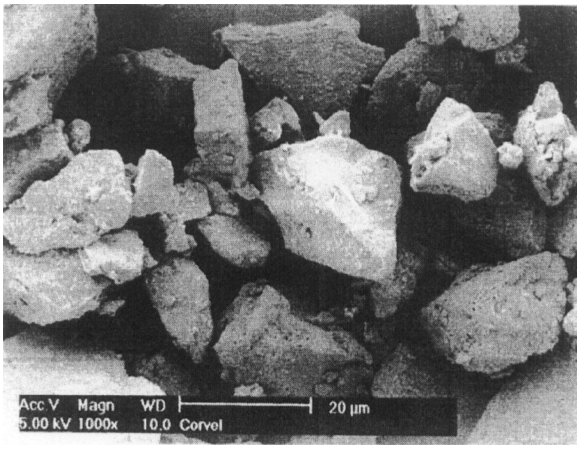

Fig. 3. SEM of epoxy powder as received.

To explore the effect of pressure drop across the nozzle and hence the effect of hydrodynamics on the system, identical experiments were performed with different nozzles. One nozzle was 180 µm in diameter and the other was 760 µm. The results shown in Fig. 7 are interesting because of the nearly identical morphologies. The implication is that jet break-up may be less significant than nucleation and growth rates at these conditions. This bodes well for increasing throughput in a scaled-up process.

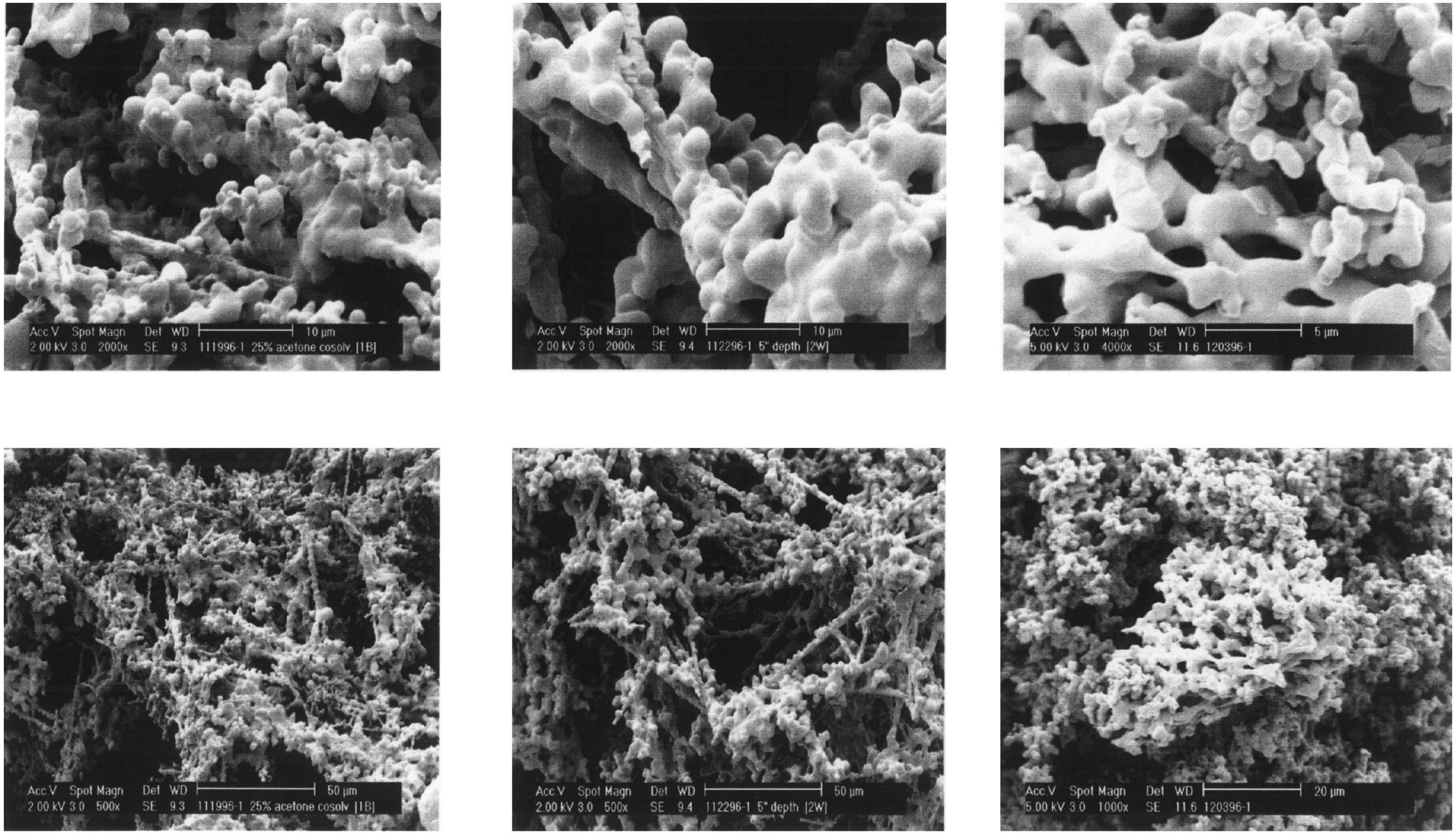

(a) (b) (c)

Fig. 4. Precipitated epoxy from acetone with varying initial concentrations: (a) 25 wt%; (b) 5 wt%; and (c) 2.5 wt%. Processing conditions were 97.6 bar, 150 µm nozzle diameter and co-current flow of CO_2 at 5–10 ml min^{-1}.

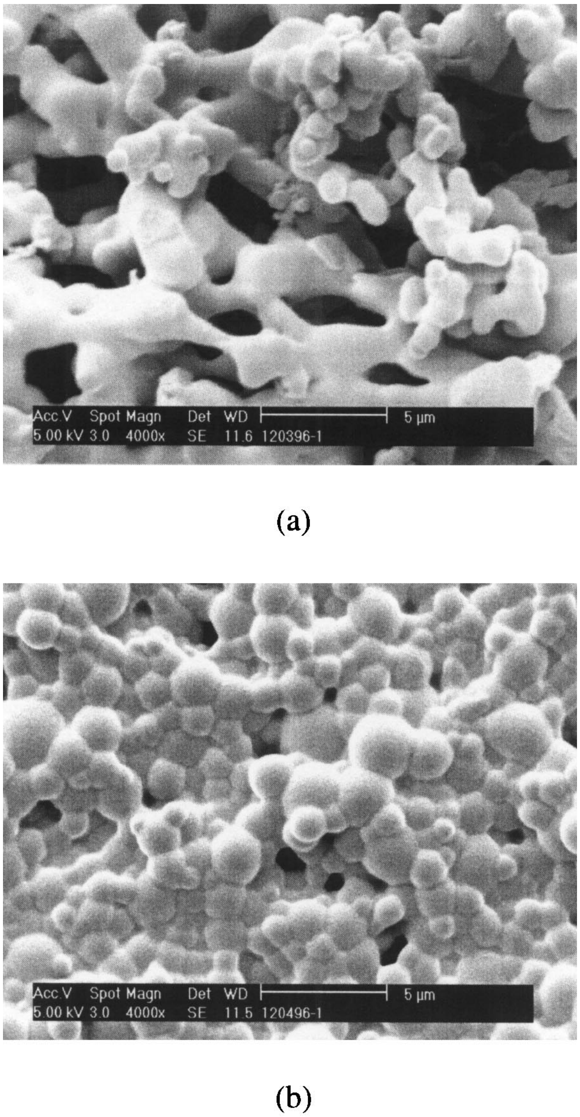

Fig. 5. Precipitated epoxy from acetone with and without surfactant present in the liquid phase: (a) no surfactant, identical to 4 (c); (b) 0.01 wt% Pluronic R-17. Processing conditions were 2.5 wt% epoxy in acetone, 97.6 bar, 150 µm nozzle diameter and co-current flow of CO_2 at 5–10 ml min^{-1}.

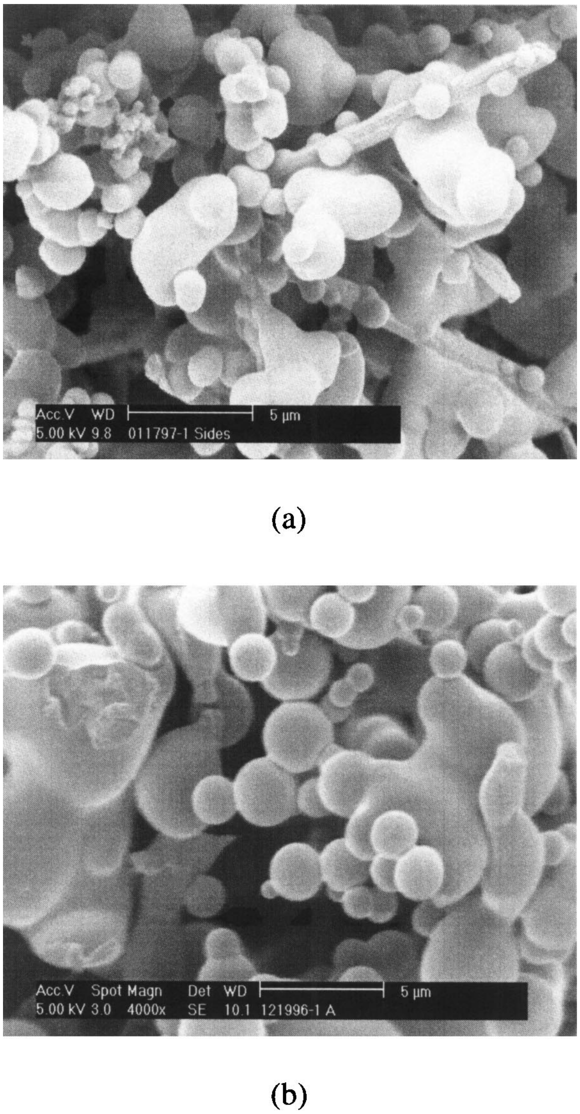

Fig. 6. Effect of processing pressure on particle morphology: (a) 63.1 bar; and (b) 97.6 bar. Processing conditions were 2.5 wt% epoxy in acetone with added surfactant, 180 µm nozzle diameter and counter-current flow of CO_2 at 5–10 ml min^{-1}.

One of the more interesting features of this study is the different result achieved with cocurrent versus countercurrent flow of CO_2. Using a countercurrent configuration resulted in significantly less bridging between particles (less agglomeration) than the cocurrent case as seen in Fig. 8. Countercurrent flow improves the formation of particles in two ways. First, it sets up a higher relative velocity between the CO_2 and the liquid jet resulting in higher shear forces and better jet break-up. Of course, in conjunction with the above discussion, and at the low flow rates of CO_2 used here (5–10 ml min^{-1} in a 2 in. ID vessel) this effect is expected to be small. Second, the mixing of the solvent and antisolvent is improved which

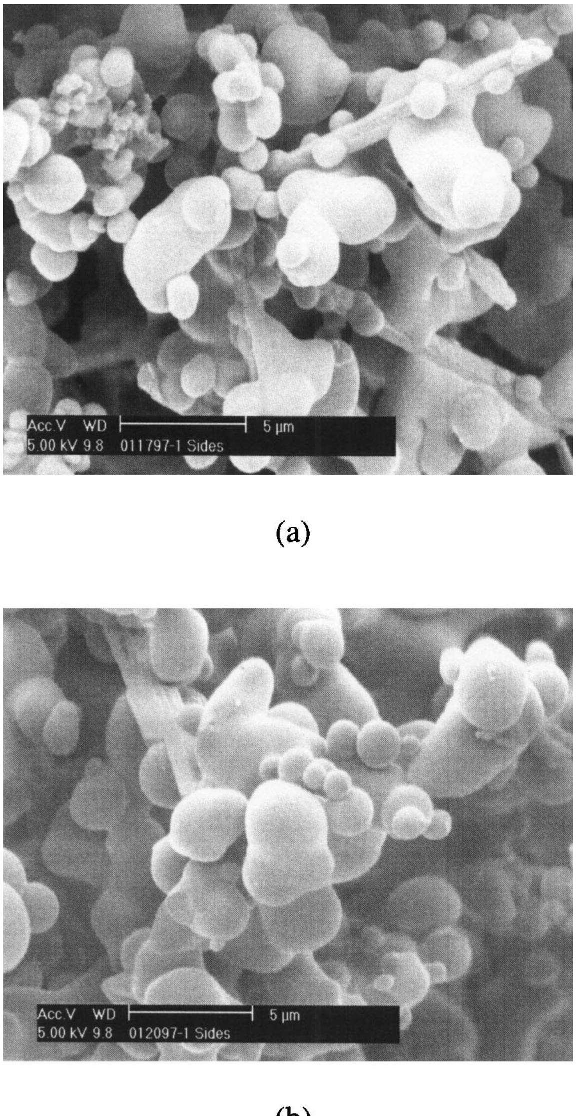

Fig. 7. Effect of nozzle size on particle morphology: (a) 180 μm diameter; and (b) 760 μm diameter. Processing conditions were 2.5 wt% epoxy in acetone with added surfactant, 63.1 bar and counter-current flow of CO_2 at 5 ml min^{-1}.

enhances the mass transfer. This mixing also gives rise to slightly larger drag forces that keep the particles suspended for a longer period of time allowing them to dry. These results provide further evidence that mass transfer has a substantial effect on particle formation and must be considered in the design of a scaled-up process.

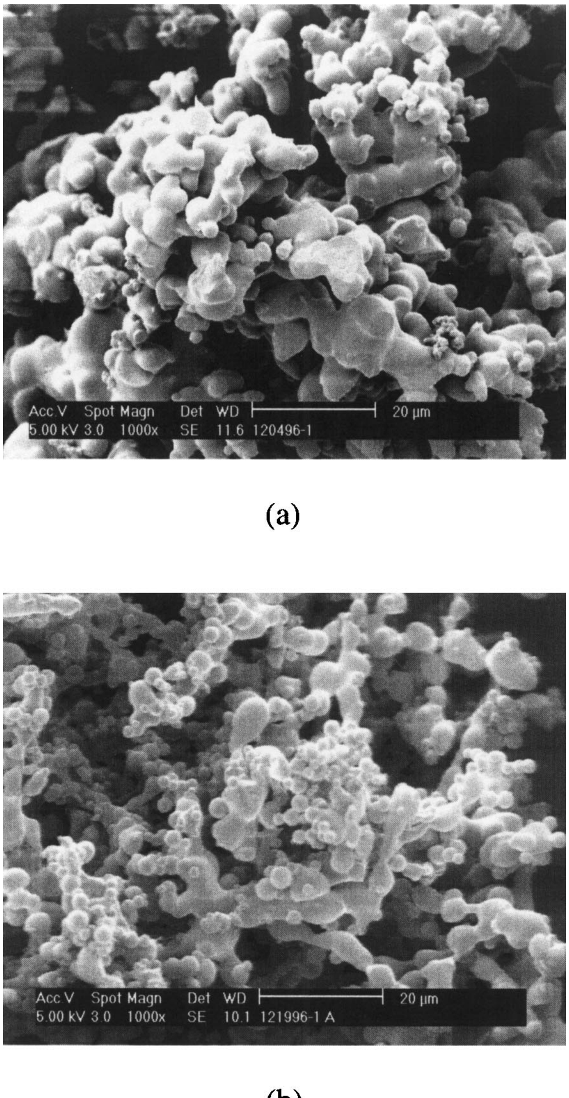

Fig. 8. Comparison of flow configuration in precipitation chamber: (a) co-current flow; and (b) counter-current flow. Processing conditions were 2.5 wt% epoxy in acetone with added surfactant, 97.6 bar, 180 μm nozzle diameter, CO_2 flow of 5–10 ml min^{-1}.

The final variable to be studied was the type of liquid solvent used. Methyl ethyl ketone (MEK) was substituted for acetone and identical experiments were performed. In general, MEK resulted in a greater predominance of spherical particles at similar conditions and the particles were smaller

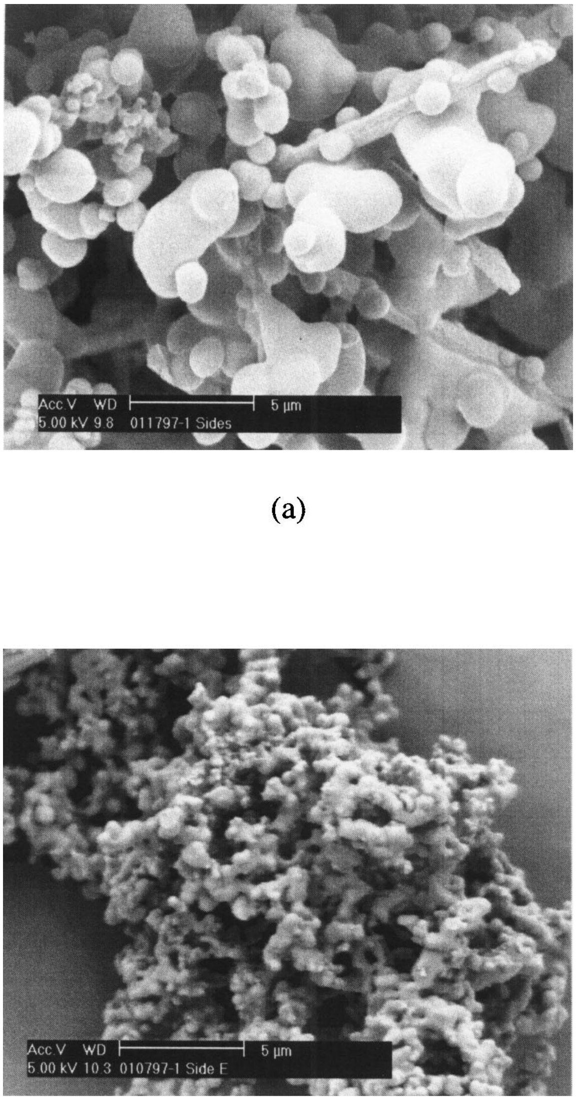

(a)

(b)

Fig. 9. Precipitated epoxy from acetone (a) and MEK (b). Processing conditions were 2.5 wt% epoxy in acetone with added surfactant, 63.1 bar, 180 µm nozzle diameter and co-current flow of CO_2 at 5–10 ml min^{-1}.

as displayed in Fig. 9. MEK has a much lower vapor pressure at 25°C (0.1333 bar) than acetone (0.2933 bar) [15]. Therefore, at the same pressure the driving force for transport of MEK into CO_2 is less than that for acetone. However, there is no reason to believe that the transport of CO_2 into MEK would be substantially different because the viscosities of the two solvents are so close. This creates a lower net rate of transport between CO_2 and MEK that may alter the mechanism of nucleation within the liquid phase. A plausible interpretation of the results in Fig. 9 is that nucleation (especially at the solvent–CO_2 interface) is

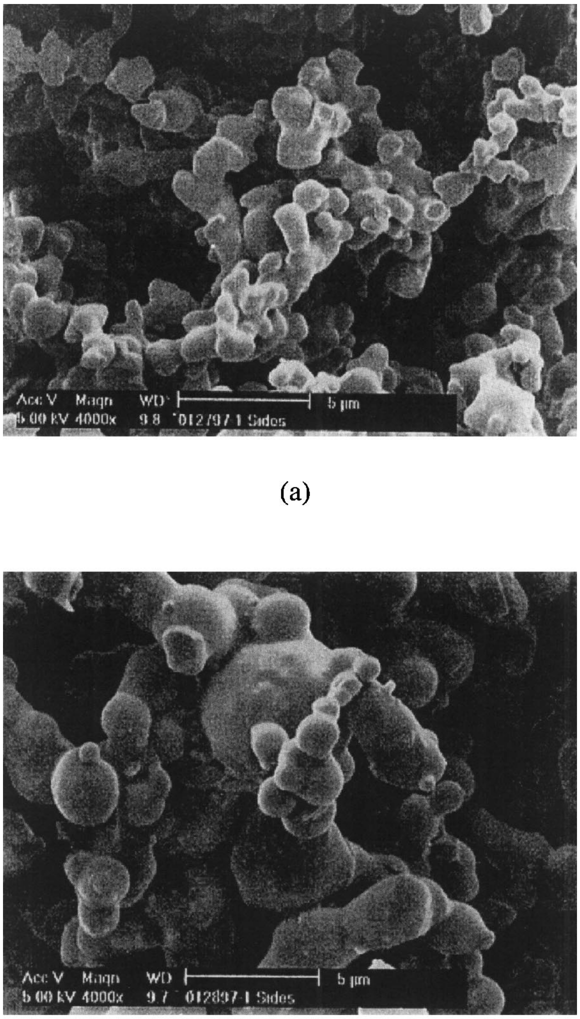

(a)

(b)

Fig. 10. Processing of high concentration polymer slurries in MEK with added surfactant (0.03 wt%): (a) 10 wt% solution at 1400 psig; (b) 25 wt% solution at 63.1 bar. Processing conditions were 180 µm nozzle diameter and counter-current flow of CO_2 at 5–10 ml min^{-1}.

delayed considerably due to slower mass transfer between CO_2 and MEK and that CO_2 transfer into the liquid (or dilation) is the primary mechanism of nucleation. This yields large porous structures that appear to be comprised of smaller particles as opposed to the acetone results which indicate a quick nucleation at the liquid surface dictates the morphology. A final issue that is not resolved by these studies is the relative affinity of the solute for MEK compared with acetone. These intermolecular interactions would also affect the nucleation rate.

One experiment was performed in which the TiO_2 pigment was included with the epoxy solution being pumped into the vessel. The particles in Fig. 10 show the characteristic rough surface topology and sharp edges indicative of the presence of inorganic material (as in Fig. 3). Note also, that the solution concentrations are much higher (10 and 25 wt%) but the predominant morphology remains spherical. This is in sharp contrast to previous work in which high solute concentrations tend to result in fibrous morphologies [6,11], but is consistent with studies on composite particles showing that polymers will tend to coat a heterogeneous nuclei to form a spherical shape [16,17].

4. Conclusions

The results indicate a few trends representative of polymers as solutes in a CO_2 antisolvent process. The relative rates of mass transfer between CO_2 and the liquid solvent dictate the onset of nucleation and the length of the growth period. In acetone, larger particles resulted from high rates of transport and nucleation occurring quickly at the solution–CO_2 interface. Conversely, with MEK as the solvent, the lower rate of mass transfer allowed nucleation to be induced by dilation of the liquid and resulted in primarily spherical morphologies but much smaller and more aggregated particles. Understanding the rates of mass transfer of CO_2 into the solvent and the solvent into CO_2 is a fundamental issue that needs to be addressed to confirm this hypothesis.

Although the hydrodynamics of jet break-up can influence particle size, it appears that it is not the dominant effect when processing polymers. More likely, issues related to nucleation rate, growth rate and mixing in the vessel dictate the final size and morphology of the particles. This conclusion is reached based on the similarity of particles from drastically different nozzle diameters and the differences in particles seen when changing the flow pattern in the vessel from cocurrent to countercurrent.

There is much to be learned about processing polymers using CO_2 antisolvent techniques. We have studied a wide range of operating conditions with an epoxy based powder coating to identify and confirm some general operating trends. Unlike many of the supercritical CO_2 based applications, this is a rate driven process and is sensitive to many parameters that have not been well documented at high pressures such as rates of mass transfer in a liquid jet in free expansion. Further work will be necessary to isolate nucleation and growth phenomena and their dependence on system parameters in this process.

Acknowledgment

This research was supported by Air Force Research Laboratory (AFRL/MLBT), Wright-Patterson AFB, OH. The prime contractor on the program was Anteon Corporation (Dayton, OH). The prime contract number was F33615-94-C-5083. The research efforts described were performed under sub-contract number 96-5803-14-11, task order number 14, of the Technical Operations Support Program.

References

[1] M.A. McHugh, T.L. Guckes, Separating polymer solutions with supercritical fluids, Macromolecules 18 (1985) 675.

[2] P.M. Gallagher, M.P. Coffey, V.J. Krukonis, N. Klasutis, GAS antisolvent recrystallization: new process to recrystallize compounds insoluble in supercritical fluids, in: K.P. Johnston, J.M.L. Penninger (Eds.), Supercritical Fluid Science and Technology, American Chemical Society, Washington, DC, 1989, p. 334.

[3] S.-D. Yeo, G.-B. Lim, P.G. Debenedetti, H. Bernstein, Formation of microparticulate protein powders using a supercritical fluid antisolvent, Biotechnol. Bioengng 41 (1993) 341.

[4] W.J. Schmitt, M.C. Salada, G.G. Shook, SpeakerS.M., III, Finely-divided powders by carrier solution injection into a near or supercritical-fluid, AIChE J. 41 (1995) 2476.

[5] E.M. Berends, O.S.L. Bruinsma, J. de Graauw, G.M. van Rosmalen, Crystallization of phenanthrene from toluene with carbon dioxide by the GAS process, AIChE J. 42 (1996) 431.

[6] T.W. Randolph, A.D. Randolph, M. Mebes, S. Yeung, Sub-micrometer-sized biodegradable particles of poly(L-lactic acid) via the GAS antisolvent spray precipitation process, Biotechnol. Prog. 9 (1993) 429.

[7] D.J. Dixon, K.P. Johnston, R.A. Bodmeier, Polymeric materials formed by precipitation with a compressed fluid antisolvent, AIChE J. 39 (1993) 127.

[8] D.J. Dixon, G. Luna-Bárcenas, K. P Johnston, Microcellular microspheres and microballoons by precipitation with a vapor–liquid compressed fluid antisolvent, Polymer 35 (1994) 3999.

[9] S.-D. Yeo, P.G. Debenedetti, M. Radosz, H.-W. Schmidt, Supercritical antisolvent process for substituted para-linked aromatic polyamides — phase equilibrium and morphology study, Macromolecules 26 (1993) 6207.

[10] S.-D. Yeo, P.G. Debenedetti, M. Radosz, R. Giesa, H.-W. Schmidt, Supercritical antisolvent process for a series of substituted para-linked aromatic polyamides, Macromolecules 28 (1995) 1316.

[11] D.J. Dixon, K.P. Johnston, Formation of microporous polymer fibers and oriented fibrils by precipitation with a compressed fluid antisolvent, J. Appl. Polym. Sci. 50 (1993) 1929.

[12] S. Mawson, K.P. Johnston, D.E. Betts, J.B. McClain, J.M. DeSimone, Stabilized polymer microparticles by precipitation with a compressed fluid antisolvent. 1. Poly(fluoro acrylates), Macromolecules 30 (1997) 71.

[13] S. Mawson, M.Z. Yates, M.L. O'Neill, K.P. Johnston, Stabilized polymer microparticles by precipitation with a compressed fluid antisolvent. 2. Poly(propylene oxide)- and poly(butylene oxide)-based copolymers, Langmuir 13 (1997) 1519.

[14] A.W. Francis, Ternary systems of liquid carbon dioxide, J. Phys. Chem. 58 (1954) 1099.

[15] R.H. Perry, D.W. Green, Chemical Engineers Handbook, 6th ed., McGraw-Hill, New York, 1984.

[16] J.W. Tom, G.-B. Lim, P.G. Debenedetti, Applications of supercritical fluids in the controlled release of drugs, in: E. Kiran, J.F. Brennecke (Eds.), Supercritical Fluid Engineering Science: Fundamentals and Applications, American Chemical Society, Washington, DC, 1993, p. 238.

[17] J.-H. Kim, T.E. Paxton, D.L. Tomasko, Microencapsulation of naproxen using rapid expansion of supercritical solutions, Biotechnol. Prog. 12 (1996) 650.